Food Chemistry: X 25 (2025) 102234

Contents lists available at ScienceDirect

Food Chemistry: X

journal homepage: www.sciencedirect.com/journal/food-chemistry-x

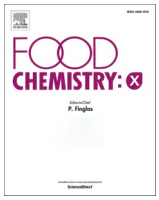

Quantitative descriptive analysis, non-targeted metabolomics and molecular docking reveal the dynamic aging and taste formation mechanism in raw Pu-erh tea during the storage

Bingsong Ma [a,b], Cunqiang Ma [a], Binxing Zhou [c], Xuan Chen [a], Yuhua Wang [a], Yifan Li [b], Junfeng Yin [b], Xinghui Li [a,*]

[a] College of Horticulture, Nanjing Agricultural University, Nanjing, 210095, Jiangsu, China
[b] Tea Research Institute Chinese Academy of Agricultural Sciences, Key Laboratory of Tea Biology and Resources Utilization, Ministry of Agriculture, 9 South Meiling Road, Hangzhou 310008, China
[c] College of Tea Science, Yunnan Agricultural University, Kunming 650201, Yunnan, China

ARTICLE INFO

Keywords:
Stored tea
Taste compounds
Aging mechanism
Molecular docking
Kokumi

ABSTRACT

Natural storage promotes raw Pu-erh tea (RaPT) aging along with chemical conversion and flavor evolution. In this study, quantitative descriptive analysis (QDA) and UHPLC-Orbitrap-MS/MS-based non-targeted metabolomics were performed to illustrate dynamic changes of taste compounds across 18 RaPT samples during the storage. Multivariate statistical analyses effectively classified stored RaPT into three groups based on storage stages, confirming that storage duration, rather than environmental conditions, primarily influences the taste profile and the changes in non-volatile compounds. A total of 509 characteristic metabolites (VIP > 1.0, $P < 0.05$, and FC > 1.50 or < 0.67) including multifarious flavor compounds related to tastes evolution were identified. Notable changes included the reduction, transformation, and condensation of flavonoids (such as catechins, flavonol glycosides, and anthocyanins) and amino acids, alongside an accumulation of organic acids, catechin/amino acid derivatives, flavoalkaloids, and gallic acid. These transformations generated significantly ($P < 0.05$) decreased umami, bitterness, and astringency, while significantly ($P < 0.05$) increasing sourness and kokumi. Molecular docking analyses further revealed that certain compounds, notably puerins and *N*-ethyl-2-pyrrolidone-substituted flavan-3-ols (EPSFs), exhibit high binding affinities with CaSR and OTOP1, contributing to the kokumi and sourness taste profiles.

1. Introduction

Pu-erh tea, a unique post-fermented tea produced from large-leaf tea species (*Camellia sinensis* (Linn.) var. assamica (Masters) Kitamura) grown in Yunnan Province of China, is favored by consumers for its mellow taste (Deng et al., 2024). Generally, Pu-erh tea could be basically divided into raw Pu-erh tea (RaPT) and ripened Pu-erh tea (RiPT) for their quality and processing differences. Besides RiPT pile-fermentation technology that was invented in the 1970s for rapid aging, natural storage is used to induce chemical transformations and reduce astringency in RaPT. (Ren et al., 2022). The higher moisture content and temperature during pile-fermentation, along with the extensive participation of a diverse microbial community, induce differences in taste, aroma, and quality ingredients between RiPT and RaPT (Wang, Qiu, et al., 2022; Yang et al., 2021). Appropriate natural storage is positively correlated with quality of RaPT, and prolonged aging is believed to enhance both its taste and market value (Lv et al., 2023). While bitterness decreases with long-term storage, complex tastes such as thickness, mouthfulness, and continuity develop, potentially explained by a kokumi taste (Li, Zhang, & Lametsch, 2022). Nowadays metabolomics (Long et al., 2020), metagenomics (Xue et al., 2020), proteomics (Zhao et al., 2019), and their integration multi-omics have elaborated pile-fermentation mechanism of RiPT (Ma et al., 2024). However, the aging mechanism of RaPT requires further investigation, particularly regarding the flavor components responsible for the kokumi characteristic taste and their dynamic changes during the storage.

Previous studies have confirmed significant decreases of most flavanols, such as (−)-epigallocatechin gallate (EGCG), amino acids, and

* Corresponding author at: College of Horticulture, Nanjing Agricultural University, Weigang No. 1, Xuanwu District, Nanjing 210095, Jiangsu Province, China.
E-mail address: lxh@njau.edu.cn (X. Li).

https://doi.org/10.1016/j.fochx.2025.102234
Received 1 December 2024; Received in revised form 15 January 2025; Accepted 24 January 2025
Available online 27 January 2025

flavonol *O*-glycosides (Xu et al., 2019), alongside the increases in gallic acid, and several non-ester catechins (Zhou, Ma, Wu, et al., 2020) during RaPT storage. In contrast, *O*-methylation of catechins, degradation of gallic acid, glycosylation of flavonoids, biosynthesis of terpenoids, and polysaccharides are found in the storage of dark teas including RiPT, Qingzhuan tea and An tea, respectively (Lv et al., 2023), which demonstrated a totally different variation tendency from RaPT storage. Enzymes secreted by microorganisms may catalyze the metabolic transformation of important amino acids and flavonoids during the storage, which further impact the taste profiles (Zhang et al., 2024).

Currently, quantitative descriptive analysis (QDA) has been developed for the objective appraisal of tea tastes and aromas, helping to elucidate flavor evolution during processing and identify relevant characteristic flavor substances (Wang et al., 2024). Additionally, ultra-high performance liquid chromatography-quadrupole time-of-flight mass spectrometry (UHPLC-Q-TOF-MS/MS) or ultra-high performance liquid chromatography-orbitrap tandem mass spectrometry (UHPLC-Orbitrap-MS/MS) approaches have been executed for non-targeted metabolomics analysis across various types of tea (Ma et al., 2021; Zhou et al., 2022). Molecular docking technology can further reveal the conformational changes and complex interactions between taste components and taste receptors (Huang et al., 2025). In this study, QDA and UHPLC-Orbitrap-MS/MS-based non-targeted metabolomics were used to analyze the correlation between the characteristic taste represented by kokumi and non-volatile compounds during RaPT storage. Molecular docking technology was also applied to further advance the understanding of the aging process and taste formation mechanisms in Pu-erh tea storage.

2. Materials and methods

2.1. Materials and reagents

Eighteen RaPT samples of six series (i.e. DZ, LC, FP, YW, MZ, and SY) were collected (Table S1 in the supplementary material), which were stored in specialized tea warehouses located in Kunming (average annual temperature of 15 °C, humidity of 60 %), and Guangzhou (average annual temperature of 22 °C, humidity of 77 %), respectively. The natural storage conditions were carefully managed to ensure that no environmental off-flavors were introduced. Specifically, based on their storage periods and the classification standards established by Zhou et al. (Zhou, Ma, Wu, et al., 2020), RaPT samples stored for up to 2 years, including DZ-X1, LC-X2, FP-X3, YW-X4, MZ-X5, and SY-X6, were defined as new tea. RaPT samples with a storage period of 3 to 7 years, including DZ-C1, LC-C2, FP-C3, YW-C4, MZ-C5, and SY-C6, were classified as aging tea. Additionally, samples stored for over 8 years, including DZ-L1, LC-L2, FP-L3, YW-L4, MZ-L5, and SY-L6, were defined as aged tea.

Monosodium glutamate (purity ≥99 %), glutathione (≥ 99 %), citric acid (≥ 99 %), sucrose (≥ 99 %), caffeine (≥ 98 %), and EGCG (≥ 98 %) were purchased from Sigma-Aldrich Co., Ltd., (St. Louis, MO, USA). Ammonium acetate, methanol and acetonitrile of LC-MS grade were purchased from CNW Technologies GmbH (Bielefeld, North Rhine-Westphalia, Germany). Ethanoic acid of LC-MS grade was purchased from Thermo Fisher Scientific (Shanghai, China).

2.2. Traditional tea sensory evaluation

Sensory evaluations were conducted by six panelists according to the Methodology for Sensory Evaluation of Tea (GB/T 23776–2018) established by China National Institute of Standardization (CNIS). Those who have undergone the training on tea sensory evaluation, and obtained the certification were selected as panelists. The evaluation procedures were as follows: a total of 150–200 g of compressed RaPT samples were prepared to assess appearance; each sample (3.0 g) was infused in 150 mL of boiling water for 2 min to evaluate liquor color, aroma, and taste. The samples were then infused again in 150 mL of boiling water for 5 min to sequentially evaluate liquor color, aroma, taste, and infused leaves. Emphasis was placed on the second infusion, with the first infusion results considered for a comprehensive assessment.

No human ethics committee or formal documentation process is available, and ethical permission to conduct a human sensory study is not a requirement in the institute. The experimental protocol followed relevant operational standards in China. Appropriate protocols were employed to protect participants' rights and privacy, including no coercion to participate, full disclosure of study requirements and risks, and informed consent obtained from all participants before the sensory evaluation.

2.3. QDA of tea tastes

QDA was conducted in a sensory panel room maintained at 21 ± 1 °C to digitally evaluate six taste qualities: umami, sweetness, sourness, bitterness, astringency, and kokumi (Li, Zhang, & Lametsch, 2022). After completing over 20 h of technical training based on the sensory evaluation criteria outlined in Table S2, six tea tasters (three males and three females, aged 22 to 45 years) were able to quantitatively distinguish sensory differences in the training solutions. Tea infusions were prepared as described in section 2.2, and approximately 5 mL of tea infusion was tasted to assess the six taste factors according to the sensory criteria, and overall coordination on a 10-point scale. Scoring criteria are as follows: 0–2: "very weak", 2–4: "weak", 4–6: "neutral", 6–8: "strong", 8–10: "very strong". Each tea sample was evaluated three times at different tasting temperatures, with a water rinse between samples.

2.4. Metabolites extraction for LC-MS/MS determination

The tea samples were form ground and collected through 40 mesh filtration for chemical determinations. And then, 20 mg of tea powder was mixed with 1000 μL of extract solution (methanol, containing isotopically-labelled internal standard mixture) for the extraction about 10 min in an ultrasonic ice-water bath after vortex mixing for 30 s (Zhou et al., 2022). After incubation for 1 h at −40 °C, the extract was centrifuged at 13,800 ×g (4 °C) for 15 min to collect the supernatant via a fresh glass vial. Quality control (QC) samples were prepared by mixing an equal aliquot of the supernatants from all samples. The supernatant was filtered by a 0.22 μm nylon membrane before LC-MS/MS analysis.

2.5. Non-targeted metabolomics analysis through UHPLC-Orbitrap-MS/MS method

The Vanquish series UHPLC system (Thermo Fisher Scientific, Waltham, MA, USA) with an ACQUITY UPLC HSS T3 column (100 × 2.1 mm, 1.8 μm; Waters Corporation, Milford, MA, USA) was developed for the UHPLC separation using 5 mmol/L ammonium acetate and 5 mmol/L acetic acid in water (A) and acetonitrile (B) as mobile phases. The elution gradient with an injection volume of 2 μL and a flow rate of 0.8 mL/min, is as follow: 0–0.5 min, 2 % B; 0.5–10.0 min, 2 %–50 % B; 10.0–11.0 min, 50 %–95 % B; 11.0–13.0 min, 95 % B; 13.0–13.1 min, 95 %–2 % B; 13.1–15.0 min, 2 % B. The autosampler temperature was 4 °C, and the column maintained at 40 °C, respectively.

The Orbitrap Exploris™ 120 high-resolution mass spectrometer (Thermo Fisher Scientific, Waltham, MA, USA) equipped with an electrospray inoization source was operated in positive (3.8 kV) and negative (−3.5 kV) modes, respectively, to acquire MS/MS spectra in the control of the acquisition software (Xcalibur, Version 4.4, Thermo). The major MS parameters have been described in our previous study (Ma et al., 2021) as following: sheath gas flow rate as 50 Arb, Aux gas flow rate as 15 Arb, capillary temperature 320 °C, and collision energy as 10/30/60. A mass scan range of *m/z* 70–1050 was applied for the full-scan MS with a resolution of 60,000 and MS/MS with a resolution of 15,000.

In-house R program was applied to peak detection,extraction, alignment, and integration. The in-house MS2 database (BiotreeDB) and public database were applied in metabolite annotation. The metabolites with a MS2 score over 0.6 were selected for non-targeted metabolomics analysis.

2.6. Molecular docking of aged characteristic compounds with taste receptors

The kokumi taste receptor, CaSR (UniProt ID: P41180) working as a homodimer (chain A and chain B) with a large extracellular Venus Flytrap (VFT) domain, which is involved in the recognition of kokumi-active molecules (Huang et al., 2025). The 3D-structure (PDB ID: 5K5S, resolution: 2.6 Å) was obtained from the RCSB Protein Data Bank (https://www.rcsb.org/). Proteins were protonated by removing water and other ligands, such as PO_4^+, Ca_2^+ and NAG prior to docking.

The sour taste receptor, OTOP1 (UniProt ID: Q7RTM1) is a protein involved in the permeation of H^+ through proton-selective ion channels to cause acidity, and homology model was performed using the AlphaFold database (https://alphafold.com) to obtain the protein structure (Dellafiora et al., 2022).

Thirty-four compounds with significant correlations ($r > 0.7$, $P < 0.01$) to the aged characteristic tastes kokumi and sourness were selected as ligands, either built using ChemDraw 22 (PerkinElmer Informatics, Inc., Waltham, MA, USA) or downloaded from the PubChem database.

Molecular docking simulations were performed using AutoDock Vina 1.1.2 (Scripps Research, USA). The receptor proteins and ligands were processed by removing water molecules, adding hydrogen atoms, and setting torsion bonds. A grid box was defined to enclose the entire protein structure. Docking simulations were run 20 times for each ligand-receptor pair, and the conformation with the highest binding score was selected as the optimal binding conformation. PyMol 2.5.5 (DeLano Scientific LLC, USA) were used to analyze and visualize the docking results.

2.7. Statistical analyses

Data are expressed as mean values with standard deviations (SD). Statistical analyses, including the independent-sample *t*-test, one-way analysis of variance (ANOVA) with Tukey's honestly significant difference (HSD) test, and bivariate correlation analysis for Pearson's correlation coefficient, were conducted using SPSS 20.0 (Armonk, NY, USA) to determine significance levels. Principal component analysis (PCA), hierarchical cluster analysis (HCA), heat map and volcano plots were performed by using Origin 9.0 software (Hampton, Massachusetts, USA). Partial least squares-discriminant analysis (PLS-DA) was performed using the Metware Cloud, a free online platform for data analysis (https://cloud.metware.cn), while orthonormal partial least squares-discriminant analysis (OPLS-DA) of metabolomic data was performed using SIMCA-P 14.0 software (Umetrics, Umeå, Sweden).

3. Results and discussion

3.1. Sensory evaluation result and taste evolution during the storage

As shown in Table S3, the liquor color, aroma, taste and infused leaves demonstrated significant differences among three storage stages of RaPT. Along with RaPT storage, tea-leaves color transformed into black-brown from dark green and yellowish-brown, and the liquor color transformed into orange red, brownish yellow or dark red from yellow-green or greenish-yellow. The fresh fragrance gradually degraded, while herbal or woody odor appeared after long-term storage. Additionally, bitterness, astringency, and umami gradually degraded and transformed into sweetness and kokumi during the storage. Generally, traditional sensory evaluation helps to differentiate new and aged RaPT based on their quality characteristics.

QDA was performed to objectively evaluate tea taste profiles using six indices, providing detailed insights into flavor evolution during RaPT warehousing. PCA (Fig. 1A) of the first two components (PC1 = 67.4 %, PC2 = 20.8 %) distinguished tea samples into three groups based on storage stages (new tea, aging tea, and aged tea) and corroborated these classifications with sensory changes over storage time. One-way ANOVA (Table S4) showed highly significant ($P < 0.01$) differences in umami, sourness, bitterness, astringency, and kokumi strength across the three groups. Specifically, new tea exhibited the highest levels of umami, astringency, and bitterness, while aged tea had the highest sourness and kokumi. The radar chart (Fig. 1B) visually illustrated taste changes over storage: a gradual decline in umami, astringency, and bitterness, alongside an increase in sourness and kokumi. Notably, sweetness remained stable ($P > 0.05$) during the storage. While previous studies have noted declines in umami and astringency with storage (Ren et al., 2022; Xu et al., 2019), this study is the first to confirm an increase in sourness and kokumi, potentially enhancing flavor quality with storage.

3.2. Metabolites profiles of RaPT in the storage

Non-targeted metabolomics were employed to explore common changes during the storage of six RaPT series stored at two different locations in this study. From 14,115 peaks detected via UHPLC-Orbitrap-MS/MS, approximately 1352 metabolites were identified with high MS1 scores and substance identification grades, classified into nine primary categories: flavonoids, organic acids, phenols, amino acids, alkaloids, sugars, lipids, phenolic acids, and terpenoids. As shown in Fig. 2A, 234 flavonoids including 84 flavanols, 58 flavonols, 22 flavones, 22 flavanones, 13 anthocyanins, 25 isoflavones, and 10 chalcones, was dominated in the metabolite profile, followed by 216 organic acids, 140 phenols, 133 lipids, 122 amino acids, 108 alkaloids, and 125 terpenoids. Additionally, 61 phenolic acids identified in RaPT, including 12 hydroxybenzoic acids, 4 hydroxyphenylacetic acids, 16 hydroxyphenylpropionic acids, 16 phenolic acid esters, and 10 tannins, influenced sourness changes during the storage. Among the 122 detected amino acids, 15 proteinogenic amino acids such as *L*-phenylalanine, L-valine, and L-arginine, along with 38 non-proteinogenic amino acids like L-theanine, showed strong correlations with umami levels in stored RaPT, while 46 amino acid derivatives and 23 peptides potentially enhanced kokumi taste over time.

During RaPT storage, significant dynamic changes occurred in major metabolite species (Fig. S1). Generally, flavonoids (primarily catechins), phenols, and phenolic acids (particularly hydroxybenzoic acids like gallic acid) are major contributors to the astringent and bitter tastes in tea infusions (Ye et al., 2022). During the storage, total flavonoid content significantly ($P < 0.05$) decreased, primarily due to reductions in flavanols such as catechins, di/tri-catechins, and catechin glycosides, while phenolic content showed only a slight decrease after more than 8 years of storage (Table S5). The significant ($P < 0.01$) accumulation of hydroxybenzoic acids led to an increase in total phenolic acid content over time. In contrast to their increase during pile-fermentation (Ge et al., 2019), hydroxyphenylacetic acids and hydroxyphenylpropionic acids remained stable during the storage.

Apart from the substantial ($P < 0.01$) decrease in flavanols, other flavonoid subclasses, such as flavonols, flavanones, isoflavones, and anthocyanins, also declined, with flavanones showing a extremely significant ($P < 0.01$) decrease after long-term storage. Flavones remained stable ($P \geq 0.05$), whereas chalcones increased significantly ($P < 0.05$), likely due to C-ring cleavage of related flavanones. Despite the relatively stable total phenolic content, specific phenolic categories, including lignans, benzofurans, and simple phenols, significantly decreased ($P < 0.05$), while coumarins and methoxyphenols increased (Table S5). The methoxyphenols was mainly derived from the *O*-methylation and oxidative condensation of phenols. While storage conditions can be likened to post-fermentation, low moisture levels limited microbial

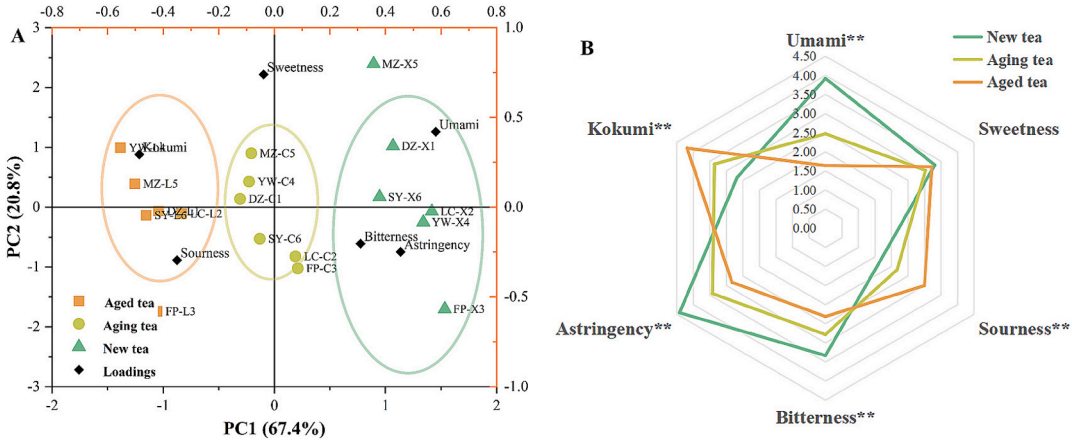

Fig. 1. Quantitative descriptive analysis achieved the classification of raw Pu-erh teas and demonstrated their taste differences. (A): Based on 6 taste index, principal component analysis (PCA) completely divided these tea samples into 3 groups, i.e. new tea, aging tea and aged tea, in accordance with their storage stages. (B): Radar map exhibited taste differences among 3 tea groups through analysis of variance (ANOVA). The symbol "**" indicates the levels of statically significant difference in $P < 0.01$.

metabolism, preserving more flavonoids and phenols in aged RaPT than in RiPT.

Apart from the substantial ($P < 0.01$) decrease in flavanols, other flavonoid subclasses, such as flavonols, flavanones, isoflavones, and anthocyanins, also declined, with flavanones showing a particularly significant ($P < 0.01$) decrease after long-term storage. Flavones remained stable ($P \geq 0.05$), whereas chalcones increased significantly ($P < 0.05$), likely due to C-ring cleavage of related flavanones. Despite the relatively stable total phenolic content, specific phenolic categories, including lignans, benzofurans, and simple phenols, significantly decreased ($P < 0.05$), while coumarins and methoxyphenols increased (Table S5). The formation of methoxyphenols was promoted by *O*-methylation and oxidative condensation of phenols. While storage conditions can be likened to post-fermentation, low moisture levels limited microbial metabolism, preserving more flavonoids and phenols in aged RaPT than in RiPT (Bian et al., 2022). The phosphorylation process, driven by microbial metabolism over prolonged storage, transforms nucleosides into nucleotides, potentially influencing sourness and umami. The continuous increase of long-chain fatty acids dominated by α-linolenic acid, isopalmitic acid and 10*E*,12*Z*-octadecadienoic acid, should be attributed to the chlorophyll decomposition (Li et al., 2023), rather than the degradation of phospholipids due to the stabilization or enhancement of glycerophospholipids during the storage.

As predominant alkaloids in tea-leaves, the purine alkaloids showed significant ($P < 0.05$) decrease during the storage. The condensation between L-theanine and catechins including ester catechins, non-ester catechins and theaflavins generated multitudinous flavoalkaloids (Li, Zhang, Wan, et al., 2022). In this study, 16 identified flavoalkaloids significantly ($P < 0.05$) increased, which might improve kokumi taste during the storage. The cyclization of amino acids such as γ-aminobutyric acid and L-theanine promoted the increase of pyrrolizidine alkaloids such as 2-pyrrolidinone (Koenig & Bonnen, 2019). Additionally, reductions in polyterpenoids degradation, such as carotenoids and luteins, significantly ($P < 0.05$) increased mono- and sesquiterpenoids (e.g. α-ionone, β-ionone, and methylionone), contributing to the woody and herbal aromas of RaPT during the storage. Gradual accumulation of organic oxygen compounds, such as alcohols and aldehydes, further influenced fragrance during the storage.

3.3. Classification and identification of stored RaPT accord with storage stages

3.3.1. PCA and HCA of metabolites for the classification of stored RaPT

The quality controls (QC) samples located in the center of PCA, confirmed the reliability of UHPLC-Orbitrap-MS/MS method for non-targeted metabolomics analysis. In the PCA (Fig. 2B), the first two components (PC1 = 34.4 % and PC2 = 10.1 %, respectively) accounted for 44.5 % of the total variance and effectively classified the RaPT samples into three distinct groups: new tea, aging tea, and aged tea. This classification suggests three stages of natural storage: short-term storage within 2 years, medium-term storage between 3 and 7 years, and long-term storage exceeding 8 years. The PLS-DA model achieved effective classification of storage stages with relatively high prediction accuracy, as indicated by $R^2X = 0.583$, $R^2Y = 0.967$, and $Q^2 = 0.819$ ($P < 0.05$, 38/1000) (Fig. S2).

These RaPT samples were generally clustered into three groups by HCA (Fig. 2C) in accordance with their storage stages. Minor sample deviations were observed, likely due to variations in storage environments. To clarify these effects, we further analyzed the differences among RaPT samples stored in distinct locations.

3.3.2. Limited impact of storage environment

The storage environment profoundly affect microbial community structure and chemical compositions in the long-term storage (Zhou, Ma, Ren, et al., 2020), which further deeply affect taste and aroma of RaPT (Shen et al., 2023; Xu et al., 2019).

The OPLS-DA model ($R^2X = 0.768$, $R^2Y = 0.975$, and $Q^2 = 0.58$, respectively) of RaPT samples stored for a certain period in Guangdong and Kunming (aging and aged stages) exhibited the impact of storage environment on metabolite profiles, and validated by 500 permutation tests (Fig. 2D, E). However, only 35 differential metabolites ($P < 0.05$ and FC > 1.50 or < 0.67) were associated with the storage environment, which confirmed that storage time is the primary factor driving metabolite changes during RaPT storage (Fig. 2F). These differential metabolites predominantly included amino acids, flavonoids (such as catechin derivatives, methoxy flavonoids, and anthocyanins), methoxy phenols, phenolic acids (including hydroxybenzoic acids), tannins, and phenolic acid esters. Comparatively, the hot and humid storage environment accelerated amino acid reduction, flavonoid glycoside hydrolysis, flavonoid and phenol *O*-methylation, and the accumulation of hydroxybenzoic acids, catechin derivatives, and flavoalkaloids over the storage period. Consistent with previous studies, storage conditions influence bacteria-fungi interactions, which affect tea metabolites through

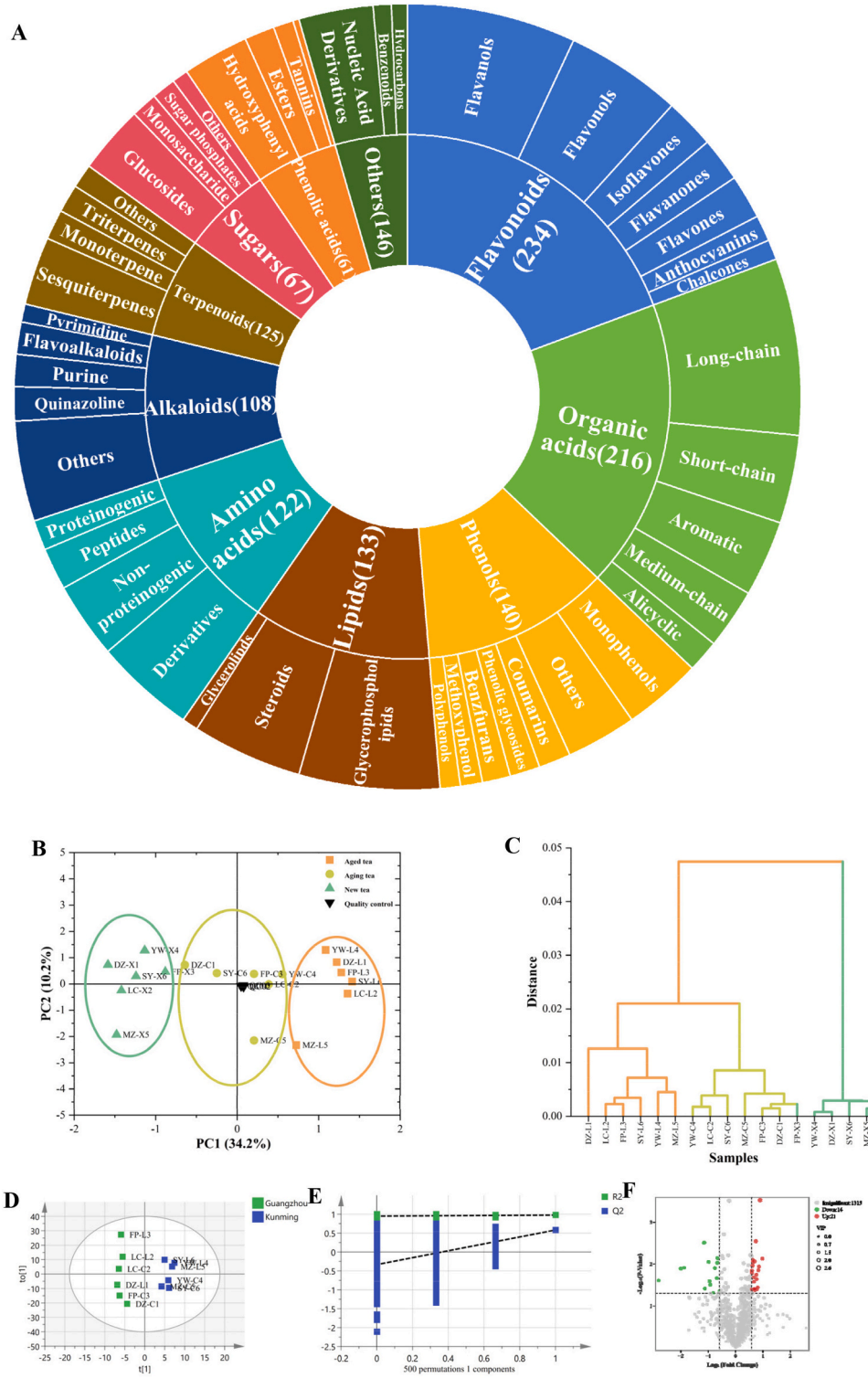

Fig. 2. Metabolites profiling of raw Pu-erh teas with various storage periods and multivariate statistical analyses. (A): Classification and quantitative distribution of 1352 metabolites. (B): Principal component analysis (PCA). (C): Hierarchical cluster analysis (HCA). (D):Volcano plots demonstrated the specific quantity of up- ($P < 0.05$ and FC >1.50) and down- (P < 0.05 and FC <0.67) regulated metabolites in storage environment (E): Orthogonal partial least squares discriminant analysis (OPLS-DA, D) indicated chemical differences in aged tea group caused by storage circumstance. (F): Volcano plots demonstrated the specific quantity of up- ($P < 0.05$ and FC >1.50) and down- ($P < 0.05$ and FC <0.67) regulated metabolites in 35 storage of environmental differential metabolites.

enzyme-catalyzed processes. Further research is needed to clarify the complex relationships between microbial communities, storage conditions, and tea metabolite pathways to optimize flavor and quality (Zhang et al., 2024).

3.3.3. *Characteristic metabolites associated with the storage stages*

The OPLS-DA (Fig. S3) comparison of different storage periods showed that 70 up-regulated ($P < 0.05$ and FC >1.50) and 246 down-regulated ($P < 0.05$ and FC < 0.67) metabolites were identified in new tea/aging tea, whereas 89 up-regulated and 120 down-regulated

metabolites were identified in aging tea/aged tea, respectively (Fig. 3A). Correspondingly, quantity and content of metabolites tended to be stable after long-term storage. In total, 509 characteristic metabolites (VIP > 1.0, $P < 0.05$, and FC > 1.50 or < 0.67) including 210 up-regulated and 299 down-regulated metabolites, were identified in new/aged storage stage (Fig. 3A). Thereinto (Fig. 3B), the relative contents of 75 metabolites including 22 organic acids, 14 phenolic compounds (i.e. 7 flavonoids, 6 phenols and 1 phenolic acid), 4 amino acids, 4 sugars and several lipids, increased by 5-folds, whereas the relative contents of 16 metabolites including 5 nucleosides/nucleotides, 4 phenolics (i.e. 3 flavonoids and 1 phenol) and 1 amino acid decreased by 5-folds after long-term storage over 8 years. Additionally, the relative contents of 169 metabolites including 40 organic acids, 37 phenolics (i.e. 20 flavonoids, 13 phenols and 4 phenolic acids), 9 sugars, 6 amino acids and 36 lipids increased over two times, while the relative contents of 98 metabolites including 21 flavonoids, 16 phenols, 4 phenolic acids, 19 amino acids, 4

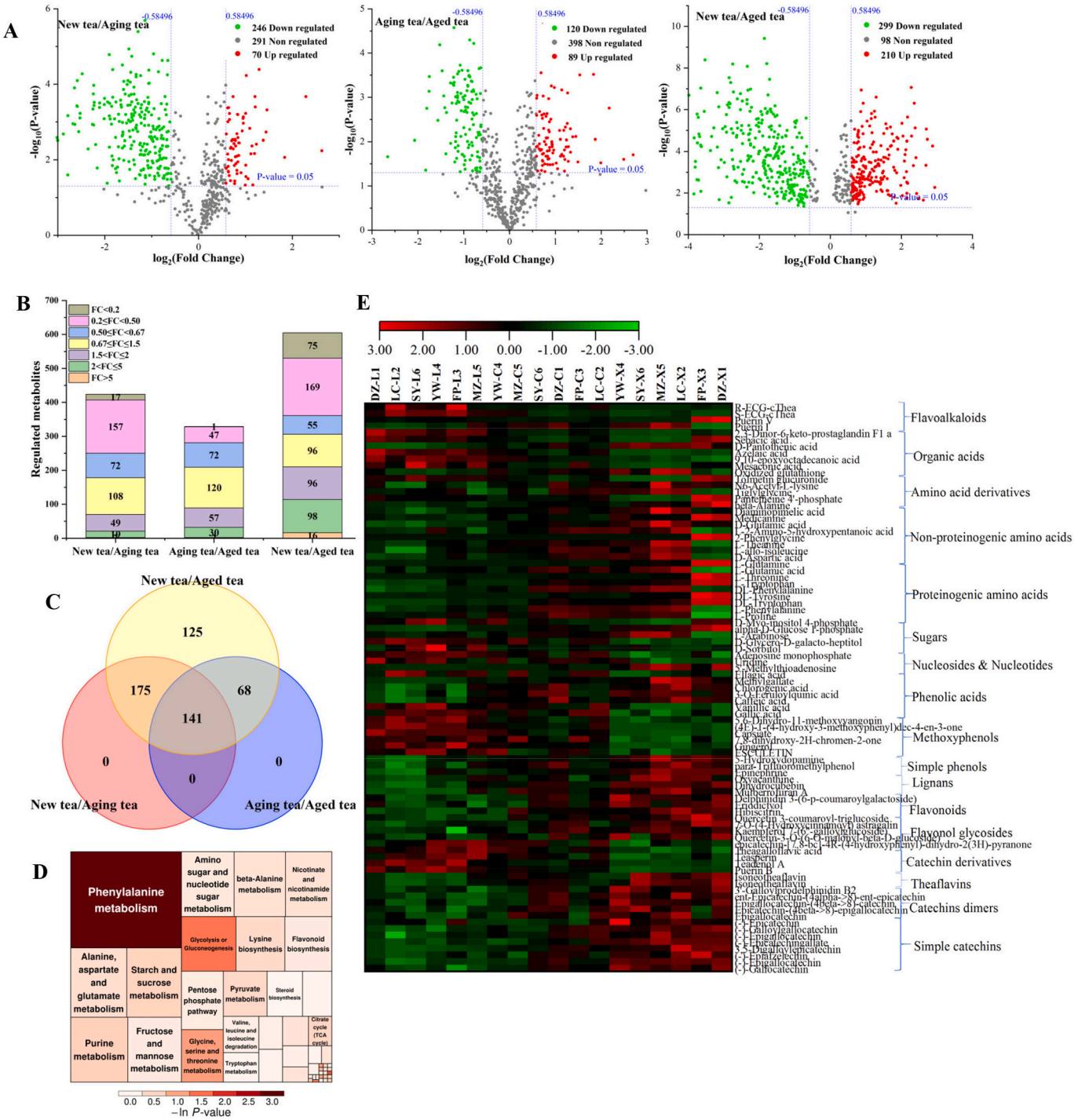

Fig. 3. Up- and down- regulated metabolites associated with the storage of raw Pu-erh tea. (A): Volcano plots demonstrated the specific quantity of up- ($P < 0.05$ and FC >1.50) and down- ($P < 0.05$ and FC <0.67) regulated metabolites in 507 selected metabolites. (B): Bar diagram showed the specific distributions of the up- and down- regulated metabolites in the 3 sets of contrastive analysis, i.e. new tea/aging tea, aging tea/aged tea, and new tea/aged tea. (C): Venn diagram indicated the formation of regulated metabolites during the storage. (D): Pathway analysis of regulated metabolites. (E): Heat map analysis indicated the dynamic changes of major regulated metabolites during the storage.

sugars and 3 organic acids reduced over a half after long-term storage over 8 years.

As shown in Fig. 3C, 175 characteristic metabolites including 47 phenolics (i.e. 22 flavonoids, 21 phenols and 4 phenolic acids), 15 amino acids, 13 sugars, 20 alkaloids, 7 nucleosides/nucleotides, 11 organic acids and 32 lipids (i.e. 18 glycerophospholipids, 4 glycerides and 10 steroids) were formulated within medium-term storage between 3 and 7 years, while 68 characteristic metabolites including 23 phenolics (i.e. 12 flavonoids, 9 phenols and 2 phenolic acids), 13 amino acids, 2 sugars, 10 organic acids and 6 lipids generated after long-term storage over 8 years. Particularly, 141 characteristic metabolites generated within medium-term storage including 32 phenolics (i.e. 16 flavonoids, 13 phenols and 3 phenolic acids), 10 amino acids, 5 sugars, 46 organic acids, 5 alkaloids, still showed significant changes after long-term storage over 8 years. Through comparisons, only 125 new differential metabolites including 53 phenolics (i.e. 33 flavonoids, 11 phenols and 9 phenolic acids), 16 amino acids, 5 sugars, 12 organic acids, 5 nucleosides/nucleotides, 7 alkaloids and 12 lipids, were found in new tea/aged tea. The metabolic pathway analysis (Fig. 3D) demonstrated the profound influence of storage process on amino acids metabolism such as phenylalanine metabolism, alanine, aspartate and glutamate metabolism and lysine biosythesis, flavonoid biosythesis and carbohydrate metabolism including amino sugar and nucleotide sugar metabolism, starch and sucrose metabolism, pentose phosphate pathway, and fructose and mannose metabolism.

3.4. Dynamic changes of taste compounds during the storage

3.4.1. Flavonoids

The gradual reduction of simple catechins (particularly ester catechins), catechin di- and trimers like proanthocyanidins, and catechin glycosides through oxidation, condensation, hydrolysis, and C-ring/B-ring fission (Fig. 3E) leads to reduced astringency and bitterness decrease during the storage. Additionally, thearubigins and theabrownins, resulting from ongoing oxidation and polymerization of theaflavins and aggregation with alkaloids, polysaccharides, proteins, and amino acids (Ma et al., 2024), are recognized as major contributors to the brownish-red color of aged teas, potentially enhancing the kokumi taste. Catechin derivatives, such as teadenol A, puerins, methyl-catechins, carboxymethyl-catechins, carboxyl-catechins, and methoxycarbonyl-catechins, exhibit increase relative content, which may influence sourness and kokumi taste. Specifically, teadenol A and teasperin derive from B-ring fission of catechins like (−)-epigallocatechin (EGC), while puerins such as puerin B result from nucleophilic reactions and condensation of non-ester catechins with organic and phenolic acids. Other catechin derivatives primarily originate from A-ring methylation, carboxylation, and methoxycarbonylation. Despite long-term storage exceeding 8 years, over 75 % of catechins, including abundant ester catechins such as EGCG, (−)-epicatechin gallate (ECG), and (−)-epigallocatechin 3-(3-methyl-gallate), are preserved in aged teas, unlike pile-fermentation, which results in the near-total loss of ester catechins like EGCG and ECG (Zhao et al., 2019). Correspondingly, the catechin di/trimers decrease by over 35 %, a comparatively higher reduction rate than simple catechins after long-term storage.

Among the detected 58 flavonols detected, including 41 flavonol glycosides, 8 simple flavonols, and 9 methoxy flavonols, these compounds are second only to flavanols in dominance among flavonoids and remain relatively stable during the storage (Table S5). Generally, the hydrolysis of flavonol glycosides such as kaempferol-, quercetin-, and myricetin-glycosides (e.g. kaempferol-3-*O*-galactoside, quercitrin, quercetin 4′-glucoside, and myricetin 3-neohesperidoside) contributes to increased levels of simple flavonols, particularly quercetin, which shows a 1.5-fold increase after long-term storage (Fig. 3E), and leads to reduced astringency. Various flavonols and flavonol glycosides found in theabrownins (Hu et al., 2022), indicated that the flavonols also participate in theabrownins formation through oxidative polymerization in the storage. Among 22 detected flavanones (including 12 flavanones, 4 flavanone glycosides, 4 dihydroflavonols, and 2 methoxyflavanones), the hydrolysis of flavanone glycosides and *O*-methylation and C-ring cleavage of flavanones/flavanonols significantly reduces 13 flavanones, to formulate methoxyflavanones such as 3′,5-dihydroxy-4′,7-dimethoxyflavanone and chalcones like phloretin, respectively. Additionally, anthocyanin hydrolysis (e.g. cyanidin-3-*O*-rutinoside chloride, malvidin 3-(6-acetylglucoside), and delphinidin 3-(6-p-coumaroylgalactoside)) increases cyanidin content during the storage. In contrast, flavone content remains stable throughout storage (Table S5), with only one flavone glycoside and one methoxy flavone assisting in identifying storage stages.

3.4.2. Phenols and phenolic acids

The 140 detected phenols fall into several sub-classes such as coumarins, lignans, benzofurans, xanthones, chromones, and simple phenols. *O*-glycosylation and hydrolysis help stabilize phenolic glycoside content throughout storage, as seen in the catalytic action of UDP glucuronosyltransferase, which may transform epinephrine into epinephrine glucuronide via *O*-glycosylation. Coumarin and chromone accumulation during the storage is linked to B-ring fission and flavonoid isomerization. *O*-methylation promote simple phenols, such as epinephrine and para-trifluoromethylphenol, into methoxyphenols, such as (4*E*)-1-(4-hydroxy-3-methoxyphenyl) dec-4-en-3-one, 5,6-dihydro-11-methoxyyangonin, and gingerol (Fig. 3E), which contribute to fragrance changes during the storage.

The total content of phenolic acids show significant ($P < 0.05$) increase during the storage. The hydroxybenzoic acids (e.g. gallic acid, 2,3-dihydroxybenzoic acid and 3,4-dihydroxybenzoic acid), and phenolic acid esters (e.g. theogallin, chlorogenic acid and 3-*O*-p-coumaroylquinic acid) dominated in the content of phenolic acids, and their mutual transformation enhanced sourness intensity during the storage (Table S5). Hydroxyphenylpropionic acids such as 4-hydroxyphenylpyruvic acid showed a slight increase during a medium-term storage, while the hydroxyphenylacetic acids contents decreased obviously during the storage. The hydrolysis of phenolic acid esters such as theogallin and chlorogenic acid, and ester catechins (i.e. ECG and EGCG) promoted the accumulation of gallic acid and caffeic acid, which could be further transformed into vanillic acid and 4-hydroxyphenylpyruvic acid through oxidation and *O*-methylation (Fig. 3E). Additionally, tannins content such as ellagic acid and chesnatin showed significant ($P < 0.05$) increase through the condensation and polymerization of gallic acid for the improvement of sourness intensity during the storage.

3.4.3. Amino acids and nucleotides

Compared with the new teas, the content of proteinogenic amino acids decreases by about 19.8 % and 40.1 %, and non-proteinogenic amino acids by 32.2 % and 55.3 % after medium- and long-term storage, respectively (Table S5), leading to reduced umami intensity. Approximately 41.45 % of L-theanine remains in aged tea after long-term storage (over 8 years), a stark contrast to pile-fermentation, which degrades L-theanine by 94.58 % (Wang, Shi, et al., 2022). While L-theanine has been reported to enhance kokumi taste in green tea infusions, its reduction during the storage confirms the generation and accumulation of kokumi-tasting compounds (Lu et al., 2022). Amino acid derivatives including *N*-acyl amino acids, *N*-methyl amino acids, hydroxy amino acids and amino acid degradation products, emerge through *N*-acylation, methylation, oxidation, and cyclization. In particular, several *N*-acyl amino acids, such as folic acid, oleoyl glycine, and *N*-acetyl-L-tyrosine (derived from *N*-acylation of glutamic acid, glycine, phenylalanine, and L-tyrosine), as well as peptides like phenylalanyl-threonine, likely contribute to kokumi taste in tea infusion. Among the 12 detected purine nucleotides, 7, such as uridine 5′-monophosphate, adenosine monophosphate, 3’-AMP, and guanosine monophosphate, significantly ($P < 0.05$) increase during the storage, potentially offsetting the umami reduction caused by amino acid

decreases (Chen et al., 2020). Notably, 5′-methylthioadenosine declines over 100-fold during the storage (Fig. 3E), degrading into adenosine and subsequently converting to adenosine monophosphate.

3.4.4. *Organic acids, sugars and purine alkaloids*

Short-chain fatty acids enhance sourness in foods (Khademi et al., 2022). However, their direct impact on tea sourness is unclear. Among 44 detected short-chain fatty acids, only 13 including 7 up-regulated and

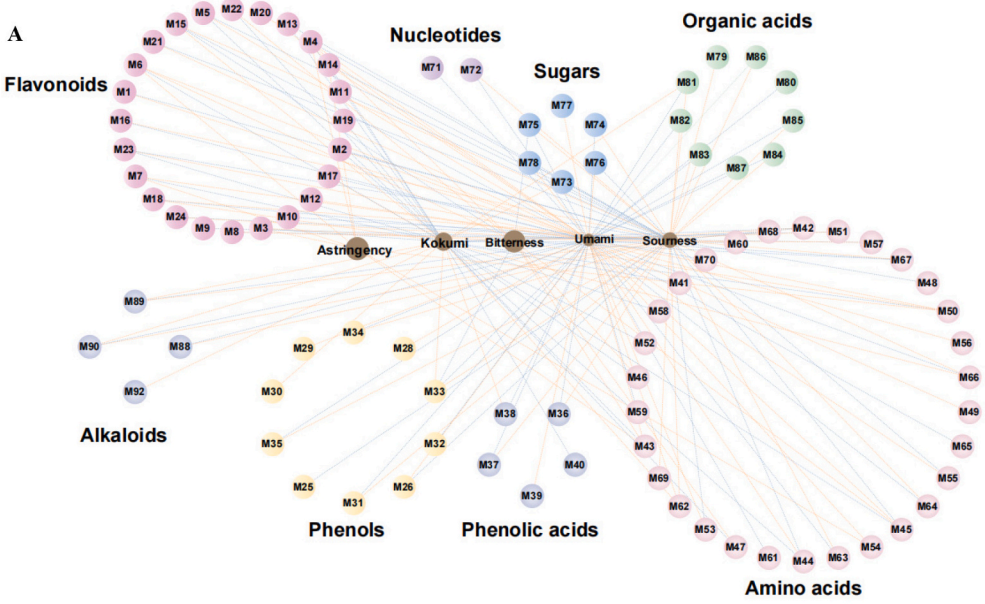

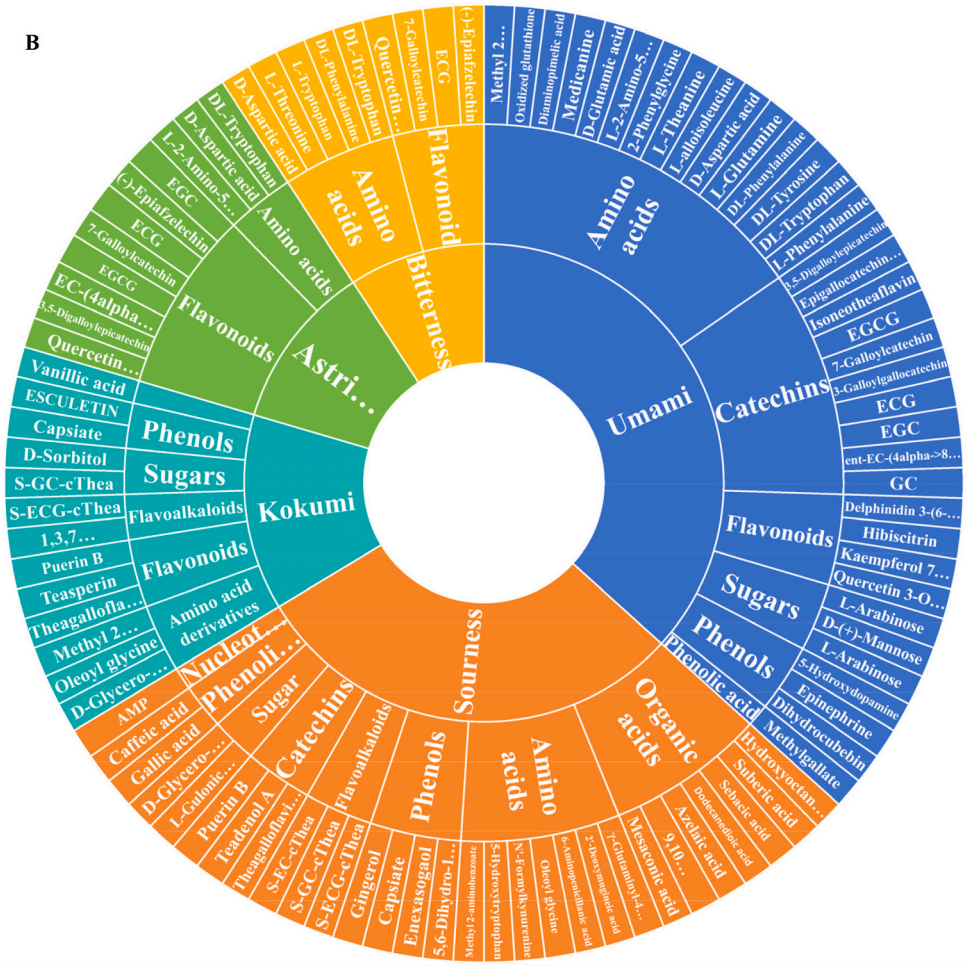

Fig. 4. Characteristic flavor compounds associated with tastes variation during the storage. (A): Correlation analysis between QDA scores and characteristic compounds in the storage. (B): Flavor wheel revealed the characteristic compounds with tastes variation during the storage.

6 down-regulated showed significant ($P < 0.05$) variations in the storage. Conversely, pile-fermentation rapidly increases short-chain fatty acids as TCA cycle intermediates (Bian et al., 2022). Significant ($P < 0.05$) increases in medium-chain fatty acids, notably 9,10-epoxyoctadecanoic acid, azelaic acid, and sebacic acid (Fig. 3E), may also influence taste during the storage.

Maltotriose, D-(+)-mannose, trehalose, sucrose, trehalose, and kojibiose dominated in RaPT, and showed significant ($P < 0.05$) differences among various series. These sugars kept relatively stable such as maltotriose, or showed an obvious decline such as sucrose during the storage. Significant ($P < 0.05$) increases in monosaccharides like D-sorbitol, (+)-perseitol, and L-gulonic gamma-lactone, alongside significant ($P < 0.05$) decreases in trehalose and L-arabinose (Fig. 3E), are observed during the storage. Additionally, terpene glycoside hydrolysis (e.g. oleuropein, perilloside C, lippioside II, and nepetariaside) produces α-terpineol, linalool, and linalool oxides, enhancing herbal or woody fragrances (Table S3). Beyond catechins, flavonol glycosides, and anthocyanins, purine alkaloids, such as caffeine, theobromine, and theophylline, significantly contribute to tea's bitterness (Ye et al., 2022). Apart from complexation and polymerization to form theabrownins and tea polysaccharides, oxidation and *N*-demethylation also decrease caffeine content during the storage, with up-regulated 1,3,7-trimethyluric acid and theophylline associated with reduced bitterness intensity.

3.5. Characteristic flavor compounds related to tastes evolution during the storage

The correlation analysis between QDA scores and metabolites was conducted to identify flavor compounds that characterize taste evolution during the storage (Table S6 and Fig. 4A). Based on their Pearson's correlation coefficients, 15 amino acids, 10 catechins, 3 flavonol glycosides, 3 sugars, 3 simple phenols and 1 phenolic acid ester were regarded as characteristic umami compounds with highly significant positive ($r > 0.7$ and $P < 0.01$) correlations, which leaded to the umami reduction for their decreases during the storage. Furthermore, the flavonoids including catechins, flavonol glycosides and anthocyanins, and amino acids such as L-tryptophan and L-threonine showed significantly positive ($r > 0.7$ and $P < 0.01$) correlations with bitterness and astringency tastes. Thereinto, 7 catechins, 1 flavonol glycoside (quercetin 3-coumaroyl-triglucoside), and 3 amino acids were linked to a decrease in astringency, with 3 catechins (ECG, 7-galloylcatechin, and (−)-epiafzelechin) and 1 flavonol glycoside also associated with bitterness. In summary, the decomposition of amino acids, the oxidative polymerization, hydrolysis, ring fission, and degradation of catechins, hydrolysis of flavonol/flavanone glycosides and anthocyanins, *O*-methylation and C-ring cleavage of flavanones, and caffeine reduction led to decreased umami, bitterness, and astringency over storage.

Organic acids, phenolic acids, catechin derivatives, amino acid derivatives, flavoalkaloids, and nucleotides showed highly significant positive correlations ($r > 0.7$, $P < 0.01$) with sourness intensity (Fig. 4A). Characteristic sourness compounds, including 7 organic acids (e.g. mesaconic acid), 2 phenolic acids (i.e. coffeic acid and gallic acid), 3 catechin derivatives, 7 amino acid derivatives, 3 flavoalkaloids, and adenosine monophosphate (AMP), contributed to the increase in sourness intensity through their accumulation during the storage (Fig. 4B). We speculate that the degradation of carbohydrates, the hydrolysis of ester catechins and phenolic acid esters, the methylation and N-acylation of amino acids, the phosphorylation of nucleosides, and the B-ring fission and condensation of catechins contribute to the enhanced sourness during storage. These metabolic changes have been demonstrated to play a key role in the increased acidity observed in black tea after prolonged storage (Zhang et al., 2023). Notably, 3 catechin derivatives (i.e. puerin B, teasperin, and theagalloflavic acid), 2 amino acid derivatives (i.e. methyl 2-aminobenzoate, and oleoyl glycine), 2 flavoalkaloids (i.e. S-GC-cThea and S-ECG-cThea) and 2 sugars (i.e. D-Glycero-D-galacto-heptitol and D-sorbitol) showed highly significantly positive ($r > 0.7$ and $P < 0.01$) correlations with kokumi taste of RaPT (Fig. 4B), which indicated that the condensation of catechins with organic acid, phenolic acids and amino acids for the generation of puerins, and flavoalkaloids enhanced the kokumi taste in the storage. Despite several kokumi-tasting compounds identified in the storage, particularly puerins, flavoalkaloids, and amino acid derivatives, the formation mechanism of kokumi taste deserves further investigation.

3.6. Kokumi and sourness taste characteristic components in aged tea by molecular docking verification

Molecular simulation technology was applied to investigate the characteristic taste compounds in aged tea associated with kokumi and sourness (Fig. 5), using 34 compounds as ligands in molecular docking studies with taste receptor proteins CaSR and OTOP1. As indicated in Table S7, the absolute docking score reflects the stability and binding strength between the ligand and receptor, with higher absolute values suggesting stronger interactions (Lao et al., 2024). All of the molecules demonstrated high affinity for both taste receptors, with binding energies below −5.0 kcal/mol (Table S7), suggesting that these compounds are likely to contribute to taste perception.

Most of the identified kokumi characteristic compounds (9/14) exhibit binding energies below −7.0 kcal/mol, indicating their strong binding affinity to CaSR receptors, which likely contributes to kokumi taste production. Surprisingly, while some studies have indicated that certain sugars and organic acids can contribute to kokumi and sourness tastes (Deng et al., 2024; Khademi et al., 2022), the binding energies from our molecular docking analysis were all above −7.0 kcal/mol, suggesting a weaker affinity. Although docking scores may not fully reflect taste intensity (Zhu et al., 2024), these results nonetheless suggest that sugars and organic acids may not be the primary compounds responsible for kokumi and sour tastes in RaPT. Additionally, we found that certain compounds demonstrated high binding affinity for both receptors. Notably, the top four compounds with binding energy to the CaSR receptor were also those identified through Pearson's correlation analysis as strongly correlated with both kokumi and sour tastes, aligning with previous findings. Interestingly, many compounds contributing to kokumi flavor are also associated with sourness taste (Li, Zhang, & Lametsch, 2022).

The binding energy of S-EC-cThea (Puerin III) to the CaSR receptor is below −9.0 kcal/mol, similar to that of S-GC-cThea (Puerin V) and S-EGC-cThea (Puerin VIII). These compounds are derivatives formed by the combination of theanine and catechins, namely 8-C *N*-ethyl-2-pyrrolidone-substituted flavan-3-ols (EPSFs), and their levels increase over storage time, potentially serving as markers of tea aging and reflecting microbial influences (Wang et al., 2014; Xie et al., 2019). Notably, these compounds share an S-type configuration, and existing research suggests that chirality may influence taste perception, although the precise mechanism remains unclear (Di Pizio et al., 2019). The formation of EPSFs has been shown to significantly reduce the bitterness and astringency of tea, and this study suggests that these compounds may also contribute to kokumi and sourness taste profiles (Jiang et al., 2022).

We conducted stress analysis on the 9 ligands with the highest binding affinity to receptors (Table 1). Among them, γ-glutaminyl-4-hydroxybenzene (GHB) is an active fungal component (Sommer et al., 2009), while teasperin and teadenol A are characteristic compounds of post-fermented tea (Geng et al., 2016; Kanegae et al., 2013). The strong binding affinity of these compounds to CaSR suggests their potential to contributions to kokumi taste, possibly influenced by microbial activity during post-fermentation in RaPT storage. However, these four compounds showed limited correlation with kokumi, which could be attributed to the diverse RaPT sampling and varying storage environments.

The force analysis showed that 26 and 13 amino acid sites were involved in the hydrogen bond formation of CaSR and OTOP1, respectively, which are important modes of action for the compounds to

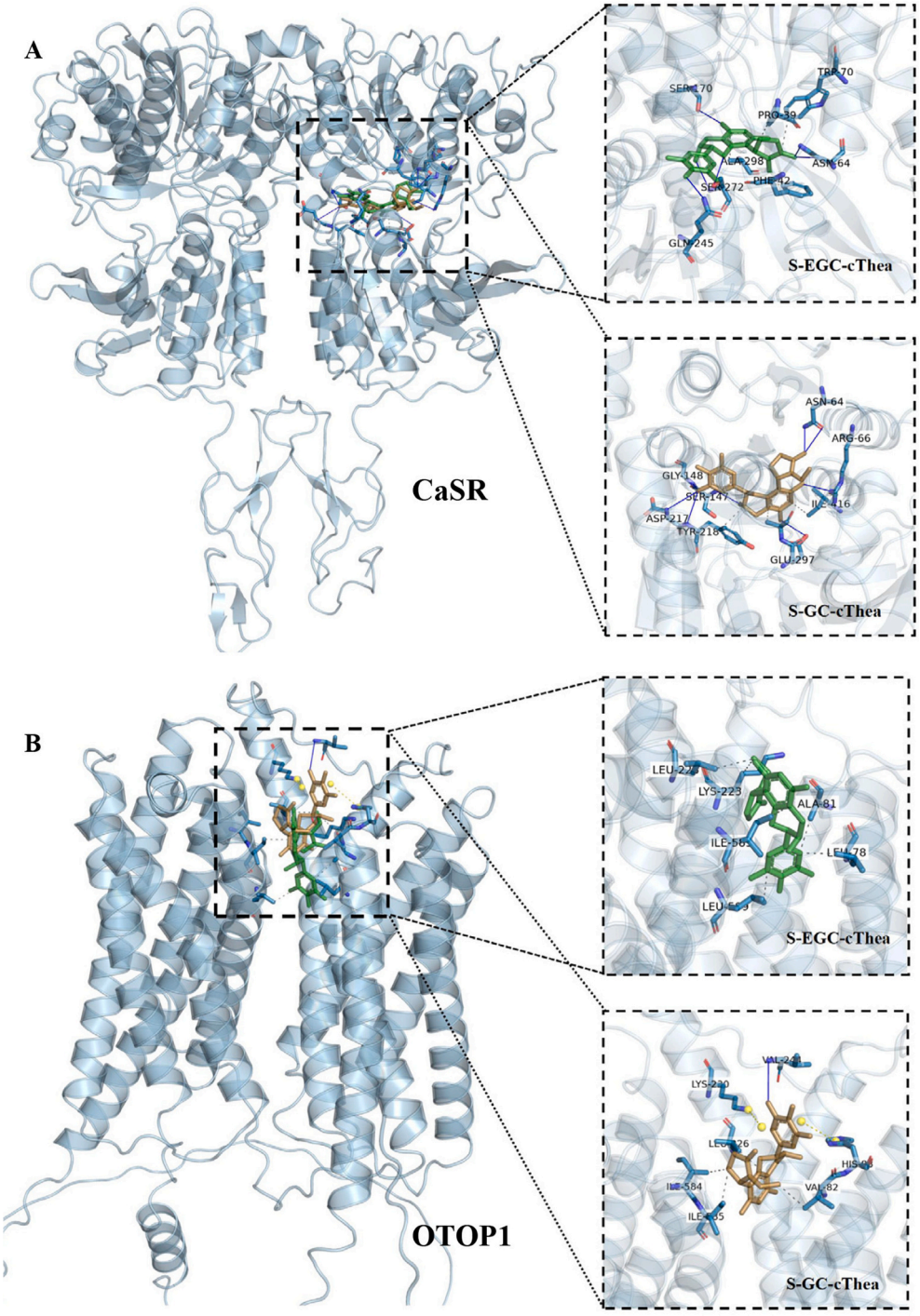

Fig. 5. Key kokumi and sourness tastes compounds interacting with taste receptors (A): Interaction of S-GC-cThea and S-EGC-cThea with the kokumi taste receptor CaSR. (B): Interaction of S-GC-cThea and S-EGC-cThea with the sour taste receptor OTOP1.

produce taste (Table 1). Consistent with previous study (Lao et al., 2024), the Arg66 was considered as a crucial binding site on the CaSR on kokumi taste compounds among these interactions. In addition, hydrophobic forces formed by hydrophobic bonds between most of molecules and the receptors, enhance the stability of the complex, assisting in the formation of taste. Certain compounds form salt bridges with the HIS and LYS residues in OTOP1, supporting the protein's 3D structure through electrostatic interactions. This mechanism may explain why S-EC-cThea and theagalloflavic acid can achieve stable binding despite having with few hydrogen or hydrophobic bonds.

4. Conclusions

Storage duration was the primary factor influencing taste evolution and chemical variation, classifying stored RaPT into three distinct stages: new tea (≤2 years), aging tea (3–7 years), and aged tea (>8 years). A total of 509 characteristic metabolites, including flavonoids, organic acids, amino acids, phenols, and phenolic acids, were identified. These metabolites were associated with reduced umami, bitterness, and astringency, while increasing sourness and kokumi, serving as markers for the respective storage stages.

During storage, catechins (including simple catechins, catechin

Table 1
Summary of the binding energy, hydrogen and hydrophobic bound amino acid between taste receptors and ligands.

Taste	Receptor	Ligands[a]	Docking score (kcal/mol)	Hydrogen bonds[b]	Hydrophobic interactions[c]/Salt Bridges[d]
Kokumi, Sour	CASR	S-ECG-cThea	−10.5	ASN64, SER170, GLN245, SER272	PRO39, PHE42, TRP70, ALA298
Kokumi, Sour	CASR	Puerin B	−9.9	SER170, GLN245, SER272	PRO39, TRP70, ASN102, TYR218, ALA298
Kokumi, Sour	CASR	S-GC-cThea	−9.5	ASN64, ARG66, SER147, GLY148, ASP217, TYR218, GLU 297	TYR218, ALA298, ILE416
Kokumi, Sour	CASR	Theagalloflavic acid	−9.5	ASN64, ARG66, ASN102, SER272, GLY273, SER303	PHE42, THR145, ALA298
Sour	CASR	S-EC-cThea	−9.3	ARG66, SER301, ARG415, ILE503	PRO407, THR412, PHE505
Sour	CASR	AMP	−8.9	ARG66, ARG69, TRP70, ALA306, THR412, HIS413, ARG415, ILE416, SER417, ILE503	/
Kokumi, Sour	CASR	Teasperin	−8.8	SER147, GLU 297, ALA298	TYR218, ILE416
Sour	CASR	GHB	−8.1	ARG66, THR145, SER147, SER170, SER272	THR145, ALA168, TYR218, ALA298, ILE416
Sour	CASR	Teadenol A	−8	ASN64, SER303, LEU304	PHE44, PRO274
Kokumi, Sour	OTOP1	S-ECG-cThea	−8.3	/	LEU78, ALA81, LYS223, LEU226, ILE585, LEU589
Kokumi, Sour	OTOP1	Puerin B	−8.2	LYS89, TYR271	PHE155, LEU162, GLU166, HIS248, TYR271
Kokumi, Sour	OTOP1	S-GC-cThea	−7.3	VAL244	VAL82, LEU226, ILE584, ILE585. HIS83[d], LYS230[d]
Kokumi, Sour	OTOP1	Theagalloflavic acid	−9	LYS89, GLU166, SER264, TYR271	/, LYS89[d]
Sour	OTOP1	S-EC-cThea	−8.6	LEU74, SER222	LEU78, LEU219, LEU226, ILE585, ASN588, LEU589
Kokumi, Sour	OTOP1	AMP	−7.8	LYS89, LYS151, GLU166, ASN216, ASN220, HIS248, TYR268	TYR154
Kokumi, Sour	OTOP1	Teasperin	−7.6	ASN220, TYR271	LYS151, TYR154, PHE155, LEU162, GLU166, PRO170
Sour	OTOP1	GHB	−7.1	LYS89, LYS151, ASN220, SER264, TYR268, TYR271	LYS151, TYR154, TYR268
Sour	OTOP1	Teadenol A	−9.1	LYS89, LYS151, TYR154, HIS248	LYS151, TYR154

[a] Nine kokumi and sourness characteristic compounds with binding energies less than −7.0 kcal/mol are shown.
[b] Key residues of OR that form hydrogen bonds, "/" No force is formed in the table.
[c] Key residues of the OR that form hydrophobic interactions, "/" No force is formed in the table.
[d] Key residues of the OR that form Salt Bridges.

dimers/trimers, theaflavins, and catechin glycosides), amino acids, flavonol/flavanone glycosides, and anthocyanins underwent transformations into derivatives like puerins, flavoalkaloids, *N*-acetyl amino acids, and peptides via oxidation, hydrolysis, condensation, and ring fission. Hydrolysis of esterified catechins and phenolic acid esters increased gallic acid levels, while *O*-methylation of phenols and flavanones promoted the formation of methoxyphenols and methoxyflavanones. Correlation analysis revealed that the significant decline in catechins, flavonol glycosides, anthocyanins, and free amino acids correlated with reduced umami, bitterness, and astringency. In contrast, the accumulation of organic acids, phenolic acids, flavoalkaloids, and catechin/amino acid derivatives, such as puerins and EPSFs, enhanced sourness and kokumi in aged tea.

Molecular docking further indicated that catechin/amino acid derivatives, especially EPSFs, demonstrated strong binding affinities to CaSR and OTOP1 receptors, contributing to kokumi and sourness. This study delineated the non-volatile variations and taste evolution during storage, along with their underlying relationships, thereby contributing to a deeper understanding of the aging mechanisms of RaPT. However, as kokumi is a characteristic taste of aged RaPT, requires further validation regarding its key flavor compounds and taste characteristics. Additionally, the influence of microbial metabolism during the storage on the formation of kokumi-active components remains unclear. Therefore, the role of storage microorganisms in the development of tea flavor warrants further investigation.

Ethics approval

No human ethics committee or formal documentation process is available, and ethical permission to conduct a human sensory study is not a requirement in the institute. The experimental protocol followed relevant operational standards in China. Appropriate protocols were employed to protect participants' rights and privacy, including no coercion to participate, full disclosure of study requirements and risks, and informed consent obtained from all participants before the sensory evaluation.

CRediT authorship contribution statement

Bingsong Ma: Writing – review & editing, Writing – original draft, Validation, Investigation, Formal analysis, Conceptualization. **Cunqiang Ma:** Writing – review & editing, Software, Methodology, Data curation. **Binxing Zhou:** Investigation, Conceptualization. **Xuan Chen:** Writing – review & editing, Supervision. **Yuhua Wang:** Writing – review & editing. **Yifan Li:** Writing – review & editing. **Junfeng Yin:** Resources, Funding acquisition, Conceptualization. **Xinghui Li:** Writing – review & editing, Project administration, Funding acquisition, Conceptualization.

Declaration of competing interest

The authors declare that they have no known competing financial interests or personal relationships that could have appeared to influence the work reported in this paper.

Acknowledgements

This research was funded by National Key Research and Development Program of China (2022YFD1601804), Innovation Project for Chinese Academy of Agricultural Sciences (CAAS-ASTIP-TRI), Central

Public-interest Scientific Institution Basal Research Fund(No. Y2024CG04), Science and Technology Projects of Nanjing (202210013), Expert Workstation of Yunnan Province (202305AF150198) and Key Research and Development Program of Sichuan Provice (2023YFN0010).

Appendix A. Supplementary data

Supplementary data to this article can be found online at https://doi.org/10.1016/j.fochx.2025.102234.

Data availability

Data will be made available on request.

References

Bian, X., Miao, W., Zhao, M., Zhao, Y., Xiao, Y., Li, N., & Wu, J.-L. (2022). Microbiota drive insoluble polysaccharides utilization via microbiome-metabolome interplay during Pu-erh tea fermentation. *Food Chemistry, 377*, Article 132007. https://doi.org/10.1016/j.foodchem.2021.132007

Chen, Q., Shi, J., Mu, B., Chen, Z., Dai, W., & Lin, Z. (2020). Metabolomics combined with proteomics provides a novel interpretation of the changes in nonvolatile compounds during white tea processing. *Food Chemistry, 332*, Article 127412. https://doi.org/10.1016/j.foodchem.2020.127412

Dellafiora, L., Magnaghi, F., Galaverna, G., & Dall'Asta, C. (2022). A mechanistic investigation on kokumi-active γ-Glutamyl tripeptides - a computational study to understand molecular basis of their activity and to identify novel potential kokumi-tasting sequences. *Food Research International, 162*, Article 111932. https://doi.org/10.1016/j.foodres.2022.111932

Deng, S. H., Zhang, T. F., Fan, S. H., Na, H. H., Dong, H. Y., Wang, B. J., … Liu, X. H. (2024). Polysaccharide Conjugates' contribution to mellow and thick taste of Pu-erh ripe tea, besides Theabrownin. *Food Chemistry-X, 23*, Article 101726. https://doi.org/10.1016/j.fochx.2024.101726

Di Pizio, A., Ben Shoshan-Galeczki, Y., Hayes, J. E., & Niv, M. Y. (2019). Bitter and sweet tasting molecules: It's complicated. *Neuroscience Letters, 700*, 56–63. https://doi.org/10.1016/j.neulet.2018.04.027

Ge, Y., Bian, X., Sun, B., Zhao, M., Ma, Y., Tang, Y., … Wu, J.-L. (2019). Dynamic profiling of phenolic acids during Pu-erh tea fermentation using derivatization liquid chromatography-mass spectrometry approach. *Journal of Agricultural and Food Chemistry, 67*(16), 4568–4577. https://doi.org/10.1021/acs.jafc.9b00789

Geng, Y., Mosyak, L., Kurinov, I., Zuo, H., Sturchler, E., Cheng, T. C., Subramanyam, P., Brown, A. P., Brennan, S. C., Mun, H.-c., Bush, M., Chen, Y., Nguyen, T. X., Cao, B., Chang, D. D., Quick, M., Conigrave, A. D., Colecraft, H. M., McDonald, P., & Fan, Q. R. (2016). Structural mechanism of ligand activation in human calcium-sensing receptor. Elife*, 5*, e13662. Doi: https://doi.org/10.7554/eLife.13662.

Hu, S., Li, X., Gao, C., Meng, X., Li, M., Li, Y., Xu, T., & Hao, Q. (2022). Detection of composition of functional component theabrownins in Pu-erh tea by degradation method. *Food Science and Human Wellness, 11*(3), 643–647. https://doi.org/10.1016/j.fshw.2021.12.021

Huang, P., Cindy, Zhao, X., & Cui, C. (2025). Discovery of N-succinyl-L-isoleucine as a novel taste enhancer via multisensory techniques and molecular simulations. *Food Chemistry, 463*, Article 141478. https://doi.org/10.1016/j.foodchem.2024.141478

Jiang, Z., Zhang, H., Han, Z., Zhai, X., Qin, C., Wen, M., … Wan, X. (2022). Study on *in vitro* preparation and taste properties of *N*-Ethyl-2-Pyrrolidinone-substituted Flavan-3-Ols. *Journal of Agricultural and Food Chemistry, 70*(12), 3832–3841. https://doi.org/10.1021/acs.jafc.2c00798

Kanegae, A., Sakamoto, A., Nakayama, H., Nakazono, Y., Yakashiro, I., Matsuo, Y., Tanaka, T., & Ishimaru, K. (2013). New phenolic compounds from *Camellia sinensis* L. fermented leaves. *Journal of Natural Medicines, 67*(3), 652–656. https://doi.org/10.1007/s11418-012-0704-5

Khademi, F., Raeisi, S. N., Younesi, M., Motamedzadegan, A., Rabiei, K., Shojaei, M., … Falsafi, M. (2022). Effect of probiotic bacteria on physicochemical, microbiological, textural, sensory properties and fatty acid profile of sour cream. *Food and Chemical Toxicology, 166*, Article 113244. https://doi.org/10.1016/j.fct.2022.113244

Koenig, M. K., & Bonnen, P. E. (2019). Metabolomics profile in ABAT deficiency pre- and post-treatment. *JIMD reports, 43*, 13–17. https://doi.org/10.1007/8904_2018_94

Lao, H., Chang, J., Zhuang, H., Song, S., Sun, M., Yao, L., Wang, H., Liu, Q., Xiong, J., Li, P., Yu, C., & Feng, T. (2024). Novel kokumi peptides from yeast extract and their taste mechanism *via* an *in silico* study. *Food & Function, 15*(5), 2459–2473. https://doi.org/10.1039/d3fo04487d

Li, J., Yuan, H., Rong, Y., Qian, M. C., Liu, F., Hua, J., … Jiang, Y. (2023). Lipid metabolic characteristics and marker compounds of ripened Pu-erh tea during pile fermentation revealed by LC-MS-based lipidomics. *Food Chemistry, 404*, Article 134665. https://doi.org/10.1016/j.foodchem.2022.134665

Li, Q., Zhang, L., & Lametsch, R. (2022). Current progress in kokumi-active peptides, evaluation and preparation methods: A review. *Critical Reviews in Food Science and Nutrition, 62*(5), 1230–1241. https://doi.org/10.1080/10408398.2020.1837726

Li, S., Zhang, L., Wan, X., Zhan, J., & Ho, C.-T. (2022). Focusing on the recent progress of tea polyphenol chemistry and perspectives. *Food Science and Human Wellness, 11*(3), 437–444. https://doi.org/10.1016/j.fshw.2021.12.033

Long, P., Wen, M., Granato, D., Zhou, J., Wu, Y., Hou, Y., & Zhang, L. (2020). Untargeted and targeted metabolomics reveal the chemical characteristic of pu-erh tea (*Camellia assamica*) during pile-fermentation. *Food Chemistry, 311*, Article 125895. https://doi.org/10.1016/j.foodchem.2019.125895

Lu, J., Cao, Y., Pan, Y., Mei, S., Zhang, G., Chu, Q., & Chen, P. (2022). Sensory-guided identification and characterization of Kokumi-tasting compounds in green tea (*Camellia sinensis* L.). *Molecules, 27*(17), Article 5677. https://doi.org/10.3390/molecules27175677

Lv, H., Feng, X., Song, H., Ma, S., Hao, Z., Hu, H., Yang, Y., Pan, Y., Zhou, S., Fan, F., Gong, S., Chu, Q., & Chen, P. (2023). Tea storage: A not thoroughly recognized and precisely designed process. *Trends in Food Science & Technology, 140*, Article 104172. https://doi.org/10.1016/j.tifs.2023.104172

Ma, C., Li, X., Zheng, C., Zhou, B., Xu, C., & Xia, T. (2021). Comparison of characteristic components in tea-leaves fermented by aspergillus pallidofulvus PT-3, aspergillus sesamicola PT-4 and Penicillium manginii PT-5 using LC-MS metabolomics and HPLC analysis. *Food Chemistry, 350*, Article 129228. https://doi.org/10.1016/j.foodchem.2021.129228

Ma, C., Ma, B., Zhou, B., Xu, L., Hu, Z., Li, X., & Chen, X. (2024). Pile-fermentation mechanism of ripened Pu-erh tea: Omics approach, chemical variation and microbial effect. *Trends in Food Science & Technology, 146*, Article 104379. https://doi.org/10.1016/j.tifs.2024.104379

Ren, Y., Hou, Y., Granato, D., Zha, M., Xu, W., & Zhang, L. (2022). Metabolomics, sensory evaluation, and enzymatic hydrolysis reveal the effect of storage on the critical astringency-active components of crude Pu-erh tea. *Journal of Food Composition and Analysis, 107*, Article 104387. https://doi.org/10.1016/j.jfca.2022.104387

Shen, S., Wu, H., Li, T., Sun, H., Wang, Y., & Ning, J. (2023). Formation of aroma characteristics driven by volatile components during long-term storage of an tea. *Food Chemistry, 411*, Article 135487. https://doi.org/10.1016/j.foodchem.2023.135487

Sommer, I., Schwartz, H., Solar, S., & Sontag, G. (2009). Effect of γ-irradiation on Agaritine, γ-Glutaminyl-4-hydroxybenzene (GHB), antioxidant capacity, and Total phenolic content of mushrooms (*Agaricus bisporus*). *Journal of Agricultural and Food Chemistry, 57*(13), 5790–5794. https://doi.org/10.1021/jf900993h

Wang, D., Shi, L., Fan, X., Lou, H., Li, W., Li, Y., Ren, D., & Yi, L. (2022). Development and validation of an efficient HILIC-QQQ-MS/MS method for quantitative and comparative profiling of 45 hydrophilic compounds in four types of tea *(Camellia sentences)*. *Food Chemistry, 371*, Article 131201. https://doi.org/10.1016/j.foodchem.2021.131201

Wang, S. A., Qiu, Y., Gan, R. Y., & Zhu, F. (2022). Chemical constituents and biological properties of Pu-erh tea. *Food Research International, 154*, Article 110899. https://doi.org/10.1016/j.foodres.2021.110899

Wang, W., Zhang, L., Wang, S., Shi, S., Jiang, Y., Li, N., & Tu, P. (2014). 8-C *N*-ethyl-2-pyrrolidinone substituted flavan-3-ols as the marker compounds of Chinese dark teas formed in the post-fermentation process provide significant antioxidative activity. *Food Chemistry, 152*, 539–545. https://doi.org/10.1016/j.foodchem.2013.10.117

Wang, Z., Gao, C., Zhao, J., Zhang, J., Zheng, Z., Huang, Y., & Sun, W. (2024). The metabolic mechanism of flavonoid glycosides and their contribution to the flavor evolution of white tea during prolonged withering. *Food Chemistry, 439*, Article 138133. https://doi.org/10.1016/j.foodchem.2023.138133

Xie, D., Dai, W., Lu, M., Tan, J., Zhang, Y., Chen, M., & Lin, Z. (2019). Nontargeted metabolomics predicts the storage duration of white teas with 8-C N-ethyl-2-pyrrolidinone-substituted flavan-3-ols as marker compounds. *Food Research International, 125*, Article 108635. https://doi.org/10.1016/j.foodres.2019.108635

Xu, S., Wang, J.-J., Wei, Y., Deng, W.-W., Wan, X., Bao, G.-H., … Ning, J. (2019). Metabolomics based on UHPLC-Orbitrap-MS and global natural product social molecular networking reveals effects of time scale and environment of storage on the metabolites and taste quality of raw Pu-erh tea. *Journal of Agricultural and Food Chemistry, 67*(43), 12084–12093. https://doi.org/10.1021/acs.jafc.9b05314

Xue, J., Yang, L., Yang, Y., Yan, J., Ye, Y., Hu, C., & Meng, Y. (2020). Contrasting microbiomes of raw and ripened Pu-erh tea associated with distinct chemical profiles. *Lwt-food. Science and Technology, 124*, Article 109147. https://doi.org/10.1016/j.lwt.2020.109147

Yang, Z. W., Miao, N., Zhang, X., Li, Q. S., Wang, Z. Q., Li, C. H., … Lan, Y. B. (2021). Employment of an electronic tongue combined with deep learning and transfer learning for discriminating the storage time of Pu-erh tea. *Food Control, 121*, Article 107608. https://doi.org/10.1016/j.foodcont.2020.107608

Ye, J.-H., Ye, Y., Yin, J.-F., Jin, J., Liang, Y.-R., Liu, R.-Y., Tang, P., & Xu, Y.-Q. (2022). Bitterness and astringency of tea leaves and products: Formation mechanism and reducing strategies. *Trends in Food Science & Technology, 123*, 130–143. https://doi.org/10.1016/j.tifs.2022.02.031

Zhang, J., Xin, W., Zou, Y., Yan, J., Tang, W., Ji, Y., & Li, W. (2024). Dynamic changes and correlation analysis of microorganisms and flavonoids/ amino acids during white tea storage. *Food Chemistry, 455*, Article 139932. https://doi.org/10.1016/j.foodchem.2024.139932

Zhang, S., Li, Q., Wen, S., Sun, L., Chen, R., Zhang, Z., Cao, J., Lai, Z., Li, Z., Lai, X., Wu, P., Sun, S., & Chen, Z. (2023). Metabolomics reveals the effects of different storage times on the acidity quality and metabolites of large-leaf black tea. *Food Chemistry, 426*, Article 136601. https://doi.org/10.1016/j.foodchem.2023.136601

Zhao, M., Su, X. Q., Nian, B., Chen, L. J., Zhang, D. L., Duan, S. M., … Ma, Y. (2019). Integrated Meta-omits approaches to understand the microbiome of spontaneous fermentation of traditional Chinese Pu-erh tea. *Msystems, 4*(6). https://doi.org/10.1128/mSystems.00680-19

Zhou, B., Ma, C., Ren, X., Xia, T., Zheng, C., & Liu, X. (2020). Correlation analysis between filamentous fungi and chemical compositions in a pu-erh type tea after a long-term storage. *Food Science & Nutrition, 8*(5), 2501–2511. https://doi.org/10.1002/fsn3.1543

Zhou, B., Ma, C., Wu, T., Xu, C., Wang, J., & Xia, T. (2020). Classification of raw Pu-erh teas with different storage time based on characteristic compounds and effect of storage environment. *Lwt-food. Science and Technology, 133*, Article 109914. https://doi.org/10.1016/j.lwt.2020.109914

Zhou, B., Wang, Z., Yin, P., Ma, B., Ma, C., Xu, C., Wang, J., Wang, Z., Yin, D., & Xia, T. (2022). Impact of prolonged withering on phenolic compounds and antioxidant capability in white tea using LC-MS-based metabolomics and HPLC analysis: Comparison with green tea. *Food Chemistry, 368*, Article 30855. https://doi.org/10.1016/j.foodchem.2021.130855

Zhu, Z., Zhang, W., Li, Z., Zhao, W., Liu, C., Zhu, B., … Yang, Q. (2024). Rethinking sweetener discovering: Multiparameter modeling of molecular docking results between the T1R2-T1R3 receptor and compounds with different tastes. *Journal of Agricultural and Food Chemistry, 72*(13), 7336–7343. https://doi.org/10.1021/acs.jafc.4c00407